

A Model for Pattern Formation on the Shells of Molluscs

HANS MEINHARDT AND MARTIN KLINGLER

Max-Planck-Institut für Entwicklungsbiologie, 7400 Tübingen, F.R.G.

(Received 9 July 1986, and in revised form 3 November 1986)

Models based on reaction-diffusion mechanisms are proposed for the generation of pigmentation and relief-like patterns on mollusc shells. They extend an earlier model to describe the formation of more complex patterns. Shell patterns are time records of a one-dimensional pattern forming process along the growing edge. Oblique lines result from travelling waves of activation (pigment production). Branches and crossings result from a temporary shift from an oscillatory into a steady state mode of pigment production. Checkerboard or meshwork-like patterns require systems with at least three components, one autocatalytic substance antagonized by two inhibitions, a diffusible inhibiting substance which generates the pattern in space and a non-diffusible one which is responsible for the pattern in time. Wavy lines, rows of dots and fish-bone like patterns can result from the superposition of two patterns: a pattern which is stable in time controls the oscillation frequency of the pigment-producing process. By computer simulations it is shown that the models reproduce not only fine details of the natural patterns but account also for pattern regulation such as observed on some species after injury.

Introduction

An extremely vivid example of the emergence of complicated patterns during development in higher organisms may be seen on the shells of molluscs. The patterns can consist of lines, stripes or patches of different pigmentations or of analogous relief-like structures like ridges and knobs. They show an enormous diversity and they are frequently of great beauty. Shells of related species can exhibit quite different patterns while non-related species can show very similar patterns. The details of the pigmentation patterns may be different even on shells of the same species. This suggests that the different patterns are generated by a common mechanism. The significance of pigment patterns for the animal itself is unclear since in many cases the animals are active at night, or live burrowed in the sand. In some cases the pigment is invisible as long as the animal is alive due to a covering of non-transparent layers. A particular pigment pattern is thus presumably without selective value, a feature which could facilitate the generation of diversity. In contrast to pigmentation patterns, relief-like patterns are believed to have a functional significance. For instance, some are used to increase friction with sand during burrowing (Seilacher, 1972, 1973). Consequently, relief-like patterns are very similar on shells of the same species.

Several attempts to model patterns on mollusc shells have been made. Formal models have been proposed by Waddington & Cove (1969) for tent-like patterns of *Olivia* shells and by Lindsay (1982) for bivalved molluscs. In an earlier paper

(Meinhardt, 1984) we described the general idea of using reaction-diffusion mechanisms to model shell patterns. A model based on similar interactions but emphasizing the role of the nervous system has been proposed by Ermentrout *et al.* (1986). In the present paper we wish to show that models formulated for primary pattern formation in higher organisms are also able to account for the formation of basic shell patterns if one takes into consideration the special geometry of the growing shell. In the main part of the paper we demonstrate that by superposition of a few elementary pattern-forming processes very complicated patterns can arise which have striking similarities with the natural patterns. We also show that the models derived from the undisturbed shell patterns provide a straightforward explanation for very non-trivial pattern regulation phenomena such as observed after injury on some shells. This provides strong support for the models proposed here. Our results suggest that pattern formation on shells may be a special application of a general mechanism of pattern formation rather than a special mechanism in itself. This makes the investigation of shell patterns more interesting since it elucidates the range of dynamic behavior of pattern forming reactions, especially if these systems are not constrained by selective pressure.

The models will be given in the form of coupled nonlinear differential equations. Computer simulations provide examples for the range of patterns which can be generated. Some computer simulations, as well as a listing of a computer program, can be found in a previous report (Meinhardt & Klingler, 1987).

Despite their mathematical formulation, our models are basically biochemical models in that they describe molecular reactions which we believe to occur in cells of the mantle edge of snails and mussels which produce the outer layer of the shell. Pigment secretion activity (or the shell secretion activity in the case of relief-bearing shells) is thought to be under the control of at least one of these substances.

The patterns on shells of most species emerge in a strict linear pattern formation process since the pattern is formed only along the growing edge of the shell. The second dimension results from growth, i.e. from the deposition of new shell material along the growing edge. The pattern on a shell is therefore a protocol of what has happened at the growing edge during the life span of the particular animal. The patterns are, therefore, space-time plots. This fact facilitates the design and testing of models since it makes geometrical simplification unnecessary. Figures 1 and 2 show a selection of typical shell patterns. It can be seen that pigmented lines are frequently oriented parallel, perpendicular or oblique relative to the direction of growth. In the latter case, as a rule, two oblique lines start at a particular point and diverge. If two such lines meet each other then both lines cease. Such lines may also branch and generate a "tent"-like pattern (Fig. 1(g)). The patterns may also consist of a more or less regular arrangement of dots or patches.

These basic types of patterns suggest that they are the results of different modes of pigment deposition. For stripes parallel to the direction of growth (i.e. usually perpendicular to the growing edge) it is sufficient that groups of cells in the mantle gland permanently secrete pigment while other groups in between never do so. Stripes parallel to the growing edge indicate that pigment production oscillates more or less synchronously in all cells, i.e. phases of pigment production alternate with periods in which no pigment production takes place.

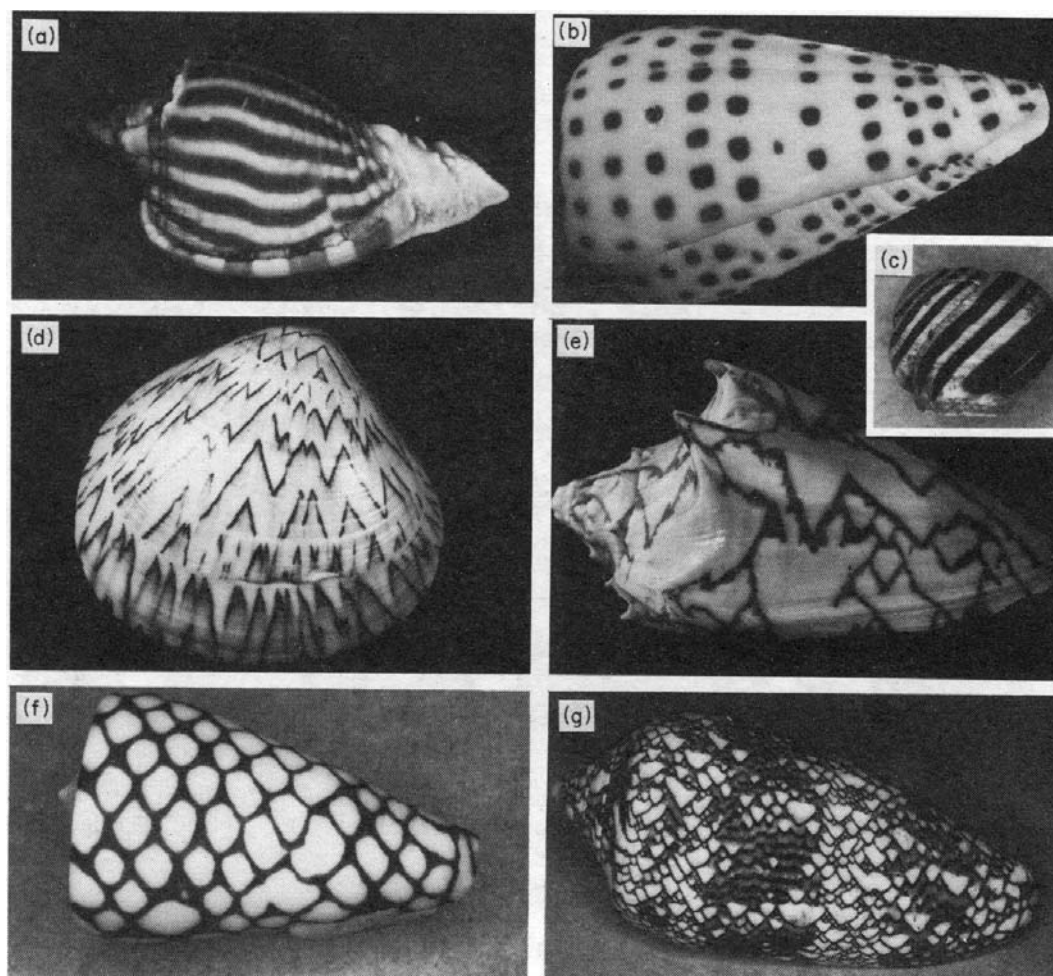


FIG. 1. Examples of pigmentation patterns. (a) Stripes parallel to the growing edge (*Phalium strigatum*). (b) Rows of patches (*Conus literatus*). (c) Stripes parallel to the direction of growth (*Cepea nemoralis*). (d) Oblique lines (*Liochoncha spec.*). (e) Oblique lines with branches (*Cymbola vespertilio*). (f) Asymmetric crossing (*Conus marchionatus*). (g) Tent-shaped pattern (*Conus textile*).

The generation of oblique lines, on the other hand, has been proposed to result from travelling waves of pigment production (Meinhardt, 1984). One pigment-producing cell "infects" a neighbour such that after some delay this cell also produces pigment and this cell in turn triggers the next neighbour, and so on. Thus, the oblique pigment lines result from long series of inductive events. In this paper we will describe a general mechanism which is capable of producing these basic patterns as well as modifications necessary to account for some more complicated patterns.

Pattern Formation in Space and Time

The modes of pigment production mentioned above indicate that the mechanism involved in shell patterning has much in common with other pattern forming systems. Oscillations and travelling waves are known to play a crucial role in the aggregation of cells of the slime mold *Dictyostelium discoideum* (Gerisch, 1968). The general situation in almost all pattern forming systems is that groups of cells develop differently to their neighbours. A classical example is head formation in the hydra.

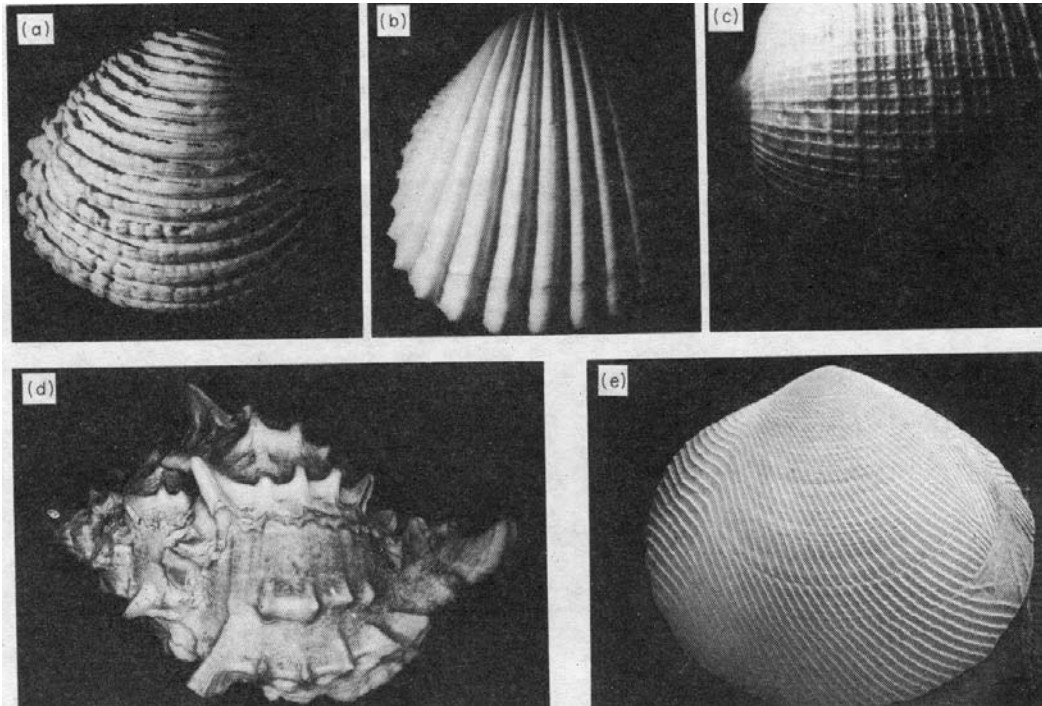


FIG. 2. Examples of relief patterns on shells. (a) Ridges parallel to the growing edges (*Venus verrucosa*). (b) Ridges parallel to the direction of growth (*Regozara anpuchese*). (c) Ridges with both orientations superimposed (*Ficus gracilis*). (d) Dent-like extrusion pattern (*Bursa ruteta*). (e) Oblique ridges (*Strigilla carnea*).

Presumably spatial pattern-forming mechanisms produce stable patterns of chemicals which determine the fate of the cells.

We have shown earlier (Gierer & Meinhardt, 1972; Meinhardt, 1982) that many pattern formation processes can be described assuming that an autocatalytic reaction is coupled with a second reaction which acts antagonistically to the autocatalysis. In the same way we assume for the shell patterning that pigment deposition or shell-bulging is under the control of a molecule, the activator a , which has—directly or indirectly—an autocatalytic feedback on its own production. The inhibitory reaction can result either from the depletion of a substrate, s , for instance a precursor necessary for the activator production, or from an inhibitor, h , which is produced simultaneously with the activator production. The mathematical formulation of these interactions can be given in the form of coupled partial differential equations. They are identical with those we have used earlier for the description of other developmental systems. A possible activator-substrate interaction is given by the following equation:

$$\frac{\partial a}{\partial t} = \rho s a^{2*} - \mu a + D_a \frac{\partial^2 a}{\partial x^2} \quad (1a)$$

$$\frac{\partial s}{\partial t} = \sigma - \rho s a^{2*} - \nu s + D_s \frac{\partial^2 s}{\partial x^2} \quad (1b)$$

where

$$a^{2*} = \frac{a^2}{1 + \kappa a^2} + \rho_0.$$

Although these equations may look complicated, they in fact describe simple molecular interactions. The activator, a , and its precursor molecule, the substrate s , diffuse from cell to cell with rates D_a and D_s respectively and decay with the rates μ and ν . The substrate is produced with the constant rate σ . Essential is that the activator production has to be an autocatalytic process and that the autocatalysis can take place only in the presence of s which is, in turn, removed during a production. It can be shown that the autocatalysis must be nonlinear (a^2) if the decay is assumed to be linear ($-\mu a$), i.e. if the decay obeys normal first order kinetics (Gierer & Meinhardt, 1972).

For the simulation of the actual shell pattern, additional features are of importance: The autocatalysis can saturate at high activator concentration, the level at which saturation is reached being controlled by the parameter κ . Since the saturation is assumed to act on the activator production as well as on the substrate depletion, saturation is subsumed in the term a^{2*} . Due to the saturation, the region of high activator concentration becomes either enlarged (Fig. 3) or, if the system oscillates, the activator pulse lasts longer.

To initiate the activator autocatalysis, a small basic, i.e. activator-independent activator production is assumed (ρ_0). This is especially of importance if the activator production oscillates. In some simulations, the general factor controlling the autocatalysis, the so-called source density ρ , has been assumed to be different from cell to cell with some random fluctuations. The fluctuation allows pattern formation in an initially homogeneous cell population, enables a different behaviour of the cells during a perturbation or demonstrates the robustness of the mechanism we propose.

Equation (2) describes an example for an interaction between an autocatalytic activator which catalyzes in addition its antagonist, the inhibitor h . The parameters are used in an analogous manner.

$$\frac{\partial a}{\partial t} = \frac{\rho(a^{2*} + \rho_0)}{h} - \mu a + D_a \frac{\partial^2 a}{\partial x^2} \quad (2a)$$

$$\frac{\partial h}{\partial t} = \rho a^{2*} - \nu h + D_h \frac{\partial^2 h}{\partial x^2} + \rho_1 \quad (2b)$$

where

$$a^{2*} = \frac{a^2}{1 + \kappa a^2}.$$

The activator-substrate model (eqn (1)) and the activator-inhibitor model (eqn (2)) lead to very similar patterns. Therefore, it is not possible to distinguish which mechanism is involved on the basis of the shell pattern. The selection of one or the other mechanism for the simulations is more or less arbitrary.

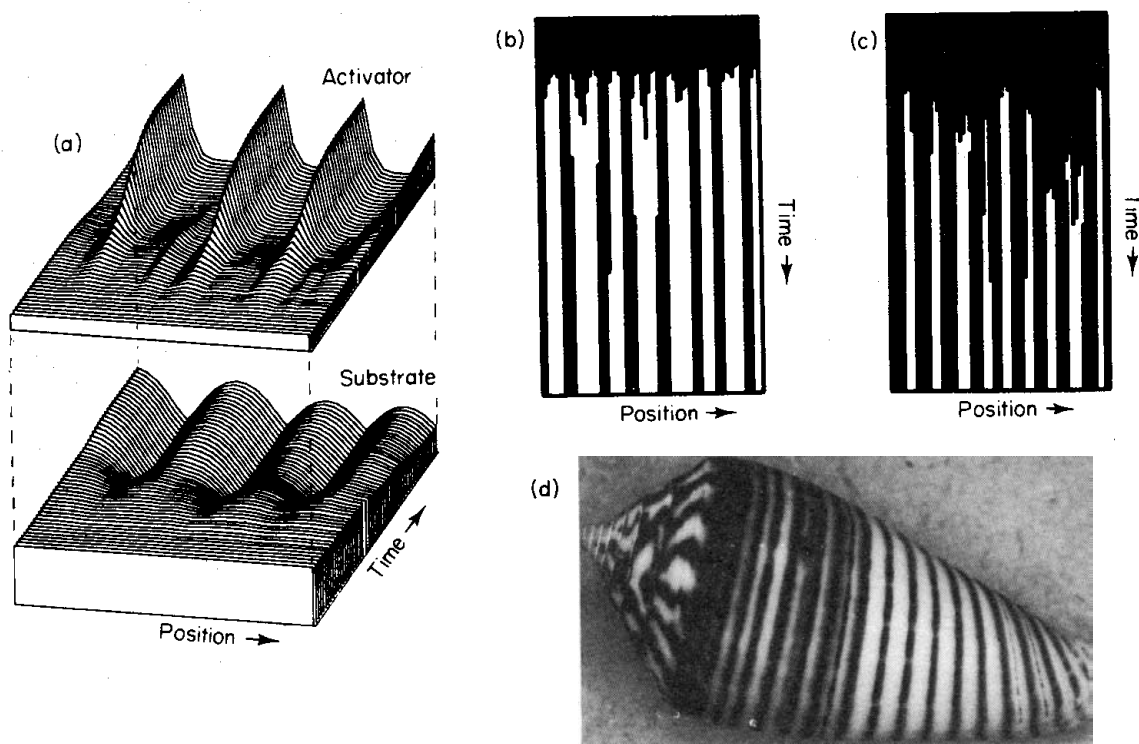


FIG. 3. Stripes parallel to the direction of growth. This pattern indicates a stable periodic pattern of pigment-producing and non-producing regions. (a) Pattern formation by the interaction of an autocatalytic activator (top) and its rapidly diffusing antagonist, in this example a diffusible substrate which is depleted during activator autocatalysis (eqn (1)). The formation of an activator maximum proceeds on expense of the substrate concentration. High activator concentration is assumed to cause pigment production. (b) Resulting pattern in a space-time plot analogous to that of shells. Regions in which the activator concentration is above a threshold are drawn in black. (c) If autocatalysis saturates, the resulting bands are broader. In this case, the maximum peak height becomes restricted. Therefore, the activated regions obtain a greater extension in order to obtain again a balance between autocatalysis and substrate depletion. Calculated with eqn (1), $\rho = 0.01 \pm \text{random fluctuations} < 2.5\%$; $\mu = 0.01$, $\rho_0 = 0.001$, $D_a = 0.002$, $\sigma = 0.015$, $\nu = 0$, $D_s = 0.4$, $\kappa = 0$ (a, b) or 0.08 (c). (d) Natural patterns: shell of *Conus macronatus*.

These equations allow us to calculate the concentration change of a , s or h in a short time interval. Adding these changes to some initial concentrations gives new concentrations at a somewhat later time. Repeating this calculation allows the computation of the complete time course of a , s and h in a row of adjacent cells. For the simulation, zero flux boundary conditions have been assumed. We will show that a variety of shell patterns can be generated by these equations. Whether synchronous oscillations, travelling waves or stationary patterns emerge depends on the time constants (μ , ν , σ) and the diffusion rates of these reactions. As shown later, more complicated patterns emerge if, for instance, one activator is antagonized by two inhibitors with different decay and diffusion rates.

Stripes Parallel to the Direction of Growth: Formation of Stable Periodic Patterns by Autocatalysis and Lateral Inhibition

As mentioned, stripes parallel to the direction of growth (and thus for most shells

perpendicular to the edge) require that some patches of cells produce pigment continuously while others never do so. Therefore, a pattern along the growing edge is required which is periodic in space but stable in time. Interactions according to eqns (1) or (2) produce such spatial periodic patterns if the antagonistic substance, the substrate s or the inhibitor h , diffuses much faster and has a shorter time constant than the autocatalytic substance a . Several stripes can be formed if the range of the inhibitory substances (depending on diffusion, decay or removal rates) is smaller than the total field, i.e. smaller than the length of the growing edge. Two parameters determine the width of a pigment line: the diffusion of the autocatalytic substance and the concentration at which its autocatalytic production saturates. Both do so in a different way such that the inspection of a pattern provides hints as to which is the critical parameter (Fig. 3).

In some species the increasing length of the growing edge cannot be neglected. The pattern forming system reacts upon growth of the field either by inserting new lines, by branching or by widening of the existing lines. The model proposed can account for these features with minor modifications of parameters (Fig. 4). In each case the ratio of pigment-producing to non-pigment-producing cells tends to remain constant at all phases of growth, consistent with observations.

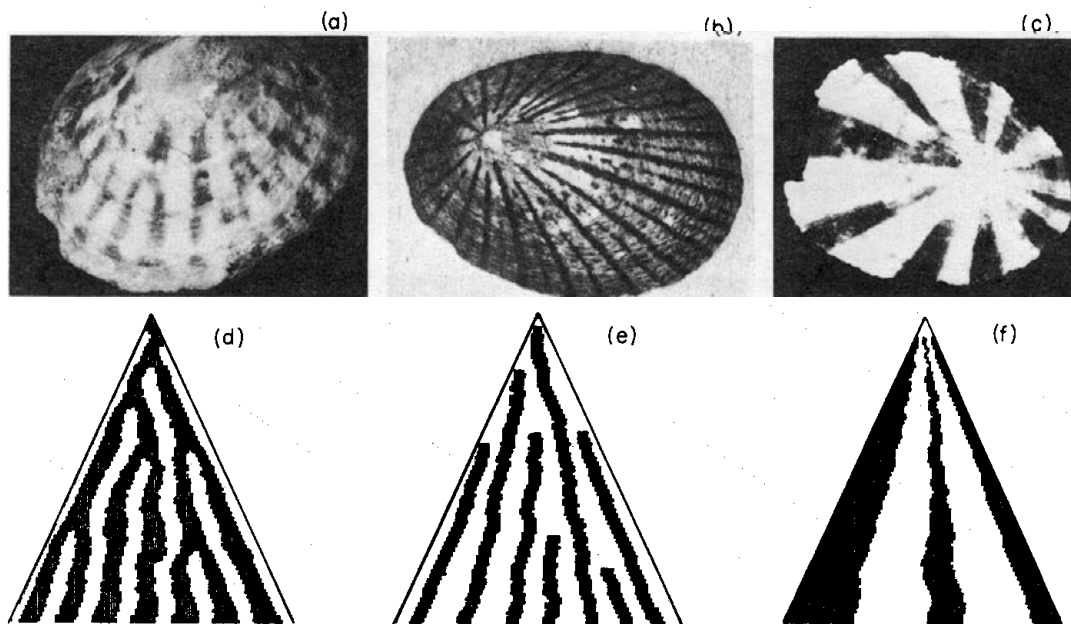


FIG. 4. Pattern regulation as consequence of growth. (a)–(c) Examples: pattern regulation can occur by bifurcation (a), by insertion of new (b) or by widening of existing pigment lines (c). (d)–(f) Computer simulations with eqn (2). Two cells are inserted at randomly selected positions after each 300 iterations. Constants used for (d): $\rho = 0.2 \pm \text{random fluctuations} < 2.5\%$, $\rho_0 = 0.01$, $\mu = 0.02$, $D_a = 0.01$, $D_b = 0.4$, $\nu = 0.02$, $\kappa = 0.15$, (e): as above except $\kappa = 0.1$, (f): as above except $\kappa = 0.4$, $D_a = 0.001$ and h is homogeneously distributed.

Stripes Parallel to the Growing Edge: Oscillating Pigment Deposition

In many species stripes more or less parallel to the growing edge are formed. This requires oscillatory pigment deposition. For stripes precisely parallel to the

growing edge the oscillations have to occur synchronously in all cells. The same equations which generate stable spatial periodic patterns, i.e. eqns (1) and (2), will also produce a pattern periodic in time, i.e. an oscillatory pattern, if the long-range of the inhibition does not belong to the space- but to the time-coordinate. In this case, the antagonist (inhibitor or precursor) does not necessarily diffuse more rapidly than the activator but has a longer time constant (i.e. oscillations will occur in eqn (1), if $\sigma < \mu$ or, in eqn (2), if $\nu < \mu$; see Meinhardt & Gierer, 1974). Then, autocataly-

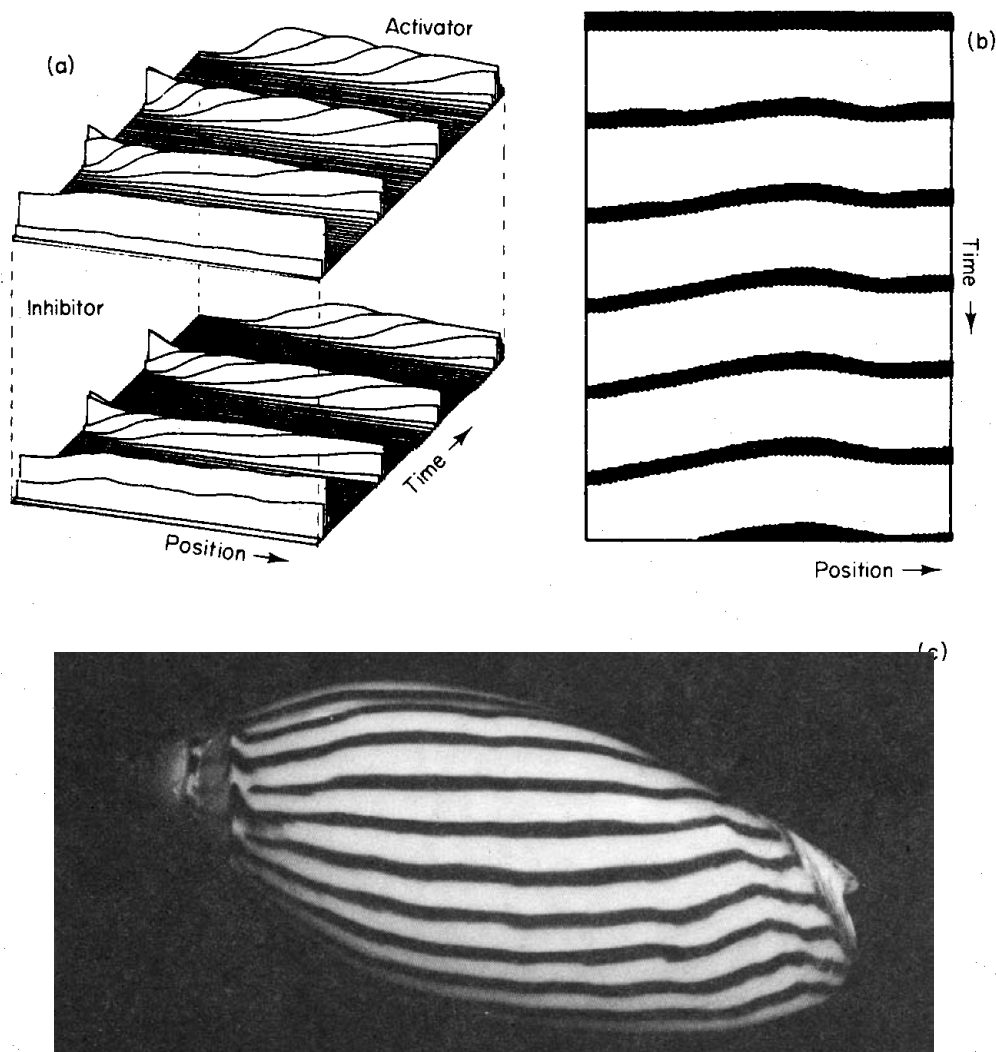


FIG. 5. Stripes parallel to the growing edge. This pattern indicates an oscillatory pigment production. (a) Model: assumed is an activator-inhibitor system (eqn (2)). The inhibitor has a longer time constant than the activator; thus, oscillations can occur. High diffusion of the activator enforces a near-synchronization between neighboring cells which causes the stripes in the final pattern. Nevertheless, despite the fact that the phase differences between neighbouring cells are small, a substantial phase difference can accumulate over the entire length of the growing edge. Calculated with eqn (2) and $\rho = 0.05 \pm$ random fluctuations $< 15\%$; $\rho_0 = 0.02$, $\kappa = 0.0004$, $\mu = 0.05$, $D_a = 0.1$, $\nu = 0.03$, $D_h = 0$ and $\rho_1 = 0.0075$. (b) A similar calculation in a space-time plot, analogous to the shell pattern. (c) Pattern on the shell of *Amoria ellioti*.

sis will proceed in a burst-like manner since, after an activator increase, the antagonistic reaction follows slowly (Fig. 5). After sufficient accumulation of inhibitor or after a severe depletion of precursor, the autocatalysis collapses and the system enters a refractory period. After a certain period of recovery, while the inhibitor has decayed or a sufficient amount of substrate has accumulated, the system again enters a sensitive phase where a new autocatalysis can be triggered by small amounts of activator. This new activation can occur spontaneously due to a basic level of activator production (ρ_0 in eqns (1) or (2)) or can be triggered by a neighbouring cell via activator diffusion (see below).

In many species, the lines are not perfectly parallel to the growing edge, indicating that the phases of oscillations in the cells of the mantle edge are to some degree independent of each other. They are not under external control such as, for instance, tree rings which emerge under seasonal influence. Activator diffusing away from a cell which has a higher activator concentration can advance the phase of a neighbouring cell. This coupling keeps neighbouring cells in approximately the same phase but over the total length of the edge a substantial phase shift can accumulate. A weaker coupling between the cells can give rise to oblique lines, as discussed in the next section.

A dot-like pattern can emerge if the conditions for lateral inhibition and for oscillations are both satisfied, i.e. if the inhibitor or the substrate have a strong diffusion and a long time constant. The resulting pattern then consists of dots, arranged in rows. However, the range of parameters which leads to this pattern is narrow and we expect that dot-like patterns arise from the superposition of two pattern forming systems. This will be discussed in more detail later.

Oblique Lines: Travelling Waves in an Excitable Medium

In many species pigmentation lines oblique to the growing edge are formed. As mentioned, this type of pattern can be regarded as a time record of travelling waves of pigment production along the edge: a cell with a high activator concentration "infects" one of its neighbours, causing, after some delay, an activator burst in this cell, and so on. If a single cell becomes spontaneously autocatalytic, it can infect both neighbouring cells. This initiates a pair of diverging lines (\wedge -element of the pattern). If, however, two travelling waves collide, all neighbouring cells are in the refractory period and therefore both waves become extinct. The result is a \vee -shaped pattern element. Travelling waves can result if the oscillation frequency is considerably different in the individual cells. The faster oscillating cells form the tip of the \wedge -shaped pattern elements since these cells can infect both neighbours. A computer simulation and, for comparison, a natural shell pattern is given in Fig. 6. To form travelling waves, the activator diffusion must be within certain ranges. If it is too high, an overall synchronization of the cells would occur and stripes more or less parallel to the edge would result (Fig. 5). On the other hand, if it is too low, the oscillations of the individual cells would be independent of each other and the phase relation among the cells would disappear (Fig. 6(b)).

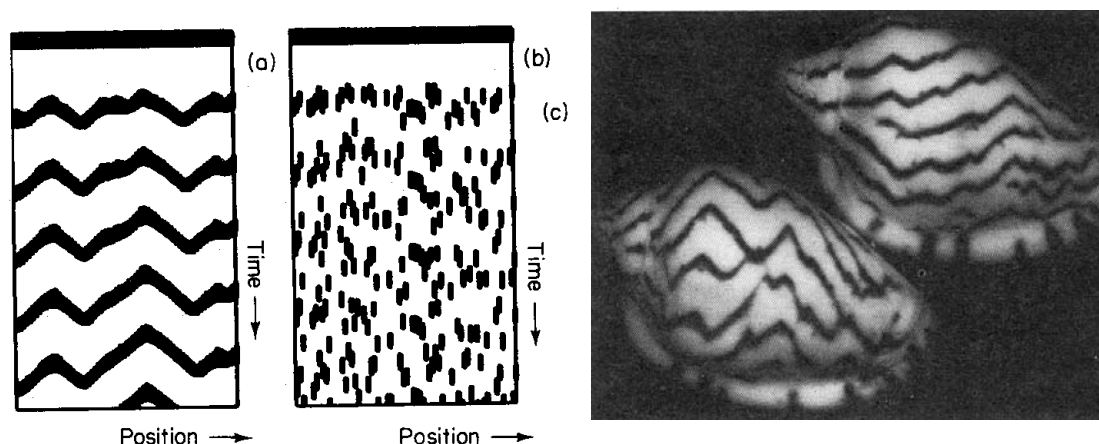


FIG. 6. Oblique lines generated by travelling waves. (a) Model: In systems with oscillatory activator production and with a limited activator diffusion, travelling waves are possible. A recently activated cell can "infect" its neighbour to become—with some delay—activated too. A chain of trigger events results. The corresponding pattern consists of lines oblique to the growing edge. The cells which oscillate somewhat faster than the average become the periodic initiation regions of two diverging lines (\wedge -elements of the pattern) since a spontaneously activated cell can infect both neighbours. At a position where two waves collide, both waves become extinct (\vee -elements of the pattern). The angle of the oblique lines is determined by the ratio of the speed of the wave and the growth rate of the shell. Calculated with the same parameters as Fig. 5 except $D_a = 0.01$. (b) In the absence of any coupling between neighbouring cells ($D_a = 0$) the phase relations in the activations are lost. The activation in each cell occurs independently of that of its neighbour and the pattern disappears. (c) Pattern on the shell of *Marginella limbata*.

Strong support for the suggestion that oblique lines are generated by travelling waves can be derived from pattern regulation processes in shells of *Strigilla carnea* (Seilacher, 1972, 1973). The normal pattern consists of very regular oblique ridges which are initiated at the left and at the right side of the shell. The ridges merge along a particular zone, producing a pattern of nested V's (Fig. 7). In some specimens, the normal pattern has been perturbed, probably by an external event. Some neighbouring lines become terminated such that a gap in the pattern is caused. Pattern regulation occurs either by a bending of the remaining lines towards the gap or by a spontaneous initiation of new lines. The computer simulation in Fig. 7 shows that the model correctly describes essential features of this pattern regulation: the bending is only in an upwards-direction resulting from a speeding up of remaining waves; a new initiation point leads to a W-like pattern, a pattern which is otherwise absent on the shell. The zone of mutual annihilation, i.e. the line formed by the tips of the V's can be shifted.

If spontaneous activation is impossible, for instance because the s -concentration does not reach the threshold due to a high s -decay rate (ν in eqn (1)), a once initiated wave will travel with a constant speed until it reaches the end of the field or until it becomes annihilated by a wave moving in the opposite direction. Then, an additional mechanism is required for wave initiation. Such a system will be discussed in the next section.

Formation of Branches on Pigmentation Lines

In many species, branches can occur along oblique pigmentation lines. Branches indicate the sudden formation of a backwards wave. The formation of a branch

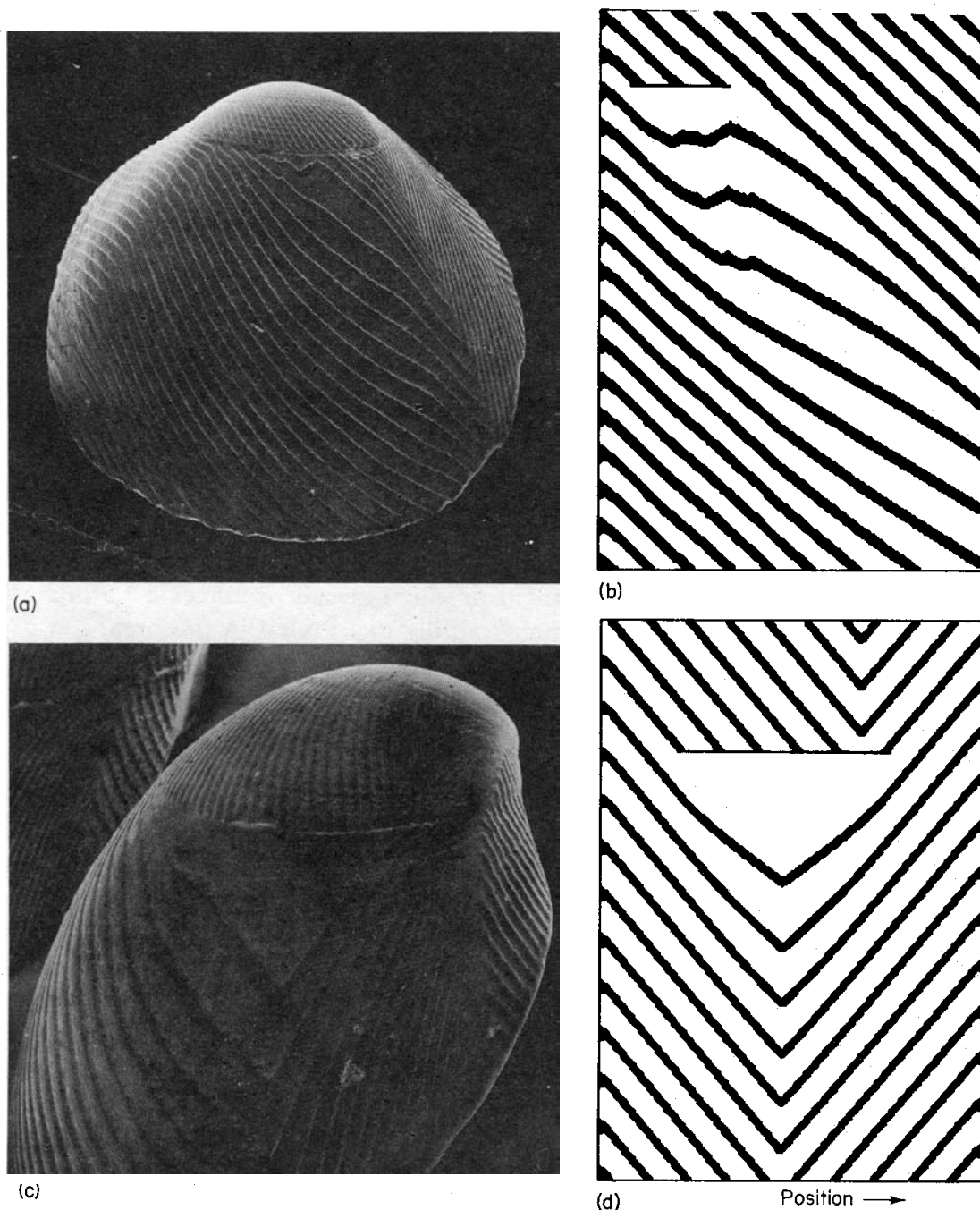


FIG. 7. Pattern regulation: repair in the rib-like pattern of *Strigilla*. The oblique rib-like pattern is assumed to be generated in a similar way as the pigmentation pattern shown in Fig. 6. Waves of increased shell secretion are initiated at the left and right "margin" of the shell. After an interruption of the normal pattern (caused presumably by an external event) regulatory processes take place which find a straight-forward explanation on the basis of the model proposed. (a) Example 1: After the interruption, lines from one side only bend towards the gap. In addition, an initiation point with two diverging lines emerges. (b) Model: after a short term lowering of the substrate concentration (to 40% of the actual concentration), the chain of trigger events is interrupted (horizontal line). Due to the absence of activation for a prolonged period, the substrate concentration (not shown) increases to such a level that a spontaneous activation becomes possible (λ -element). The bending indicates a higher speed of the travelling waves. Due to the accumulating substrate, the cells become more and more susceptible to the trigger from neighbouring cells. This leads to a speeding up of the travelling waves. The bending is unilateral since the waves on the other side of the gap are, of course, not retarded. (c) Example 2: The gap includes the annihilation zone (ν -elements). A new annihilation zone is formed at a different position. (d) Model: If the gap is asymmetrically located in respect to the normal annihilation zone, the new region of annihilation is shifted accordingly. This supports the view that the position of the nested V's is determined by the collision of waves and not by a special positional information. The model describes also correctly that, if the gap includes the former zone of collision, a bending of the ridges at both sides of the gap takes place. Calculated with eqn (1), $\rho = 0.5$, $\kappa = 1$, $\mu = 0.1$, $D_a = 0.02$, $\rho_0 = 0.0006$, $\nu = 0$, $D_h = 0$, $\sigma = 0.015 \pm \text{random fluctuations} < 15\%$. To initiate the V-pattern, $\sigma = 0.045$ has been assumed for the left and right boundary cell.

requires, for a short period, a modification of the simple serial trigger mechanism that generates the oblique lines. A particular cell, or group of cells, has to remain activated for a prolonged period such that its activation "survives" the refractory period of its earlier activated neighbour. After this refractory period a backwards infection is possible which initiates the backwards wave. Thus, the formation of branches requires two additional features: a signal must be available to cause a branch to form and, secondly, this signal must cause an elongation of the activation period. What can the signal be? As mentioned, if two travelling waves collide, both become extinguished. Thus, the number of travelling waves present along the growing edge would become smaller with each collision. A way to compensate for this loss is to form new branches. This suggests that the signal for branch formation is formed whenever the number of travelling waves becomes lower than a certain threshold. A measure of how many travelling waves are present could be obtained in the following way: each activated (pigment-producing) cell produces a hormone-like regulatory substance R which becomes rapidly distributed in the organism. Consequently, the concentration of R decreases with a decreasing number of travelling waves. Branch formation should be initiated if the concentration of R drops below a critical value.

To initiate branch formation at low R concentration it is necessary to change the newly activated cells from the oscillatory mode to a steady state activator production. As a consequence, the newly activated cells remain activated and when the refractory period of the neighbouring cell is over, the backwards infection becomes possible. Hence the number of travelling waves increases and along with the concentration of R . This has the consequence that the steady state activation becomes unstable. All cells switch back to the oscillatory mode. Thereafter, oblique lines, including those just initiated by branch formation, are elongated by the normal chain of trigger events.

How can R control the shift between the oscillatory and steady state activator production? In the activator-inhibitor model (eqn (2)), as mentioned, the activation oscillates if the inhibitor decay is slower compared with the activator decay, i.e. if $\nu < \mu$ but remains in a steady state if $\nu > \mu$. If the inhibitor decay is inhibited by R (i.e. if in eqn (1) ν is substituted by ν/R), a low R concentration leads to high inhibitor decay and thus to a shift into the steady state activator production and to branch formation. Figure (8) shows a simulation and a natural pattern. The global control of branching via a hormone has the consequence that branches occur simultaneously along many oblique lines—a feature which is in agreement with the pattern on shells of *Olivia porphyria* (Figs 8(a) and (b)).

With this regulation, the number of travelling waves along the growing edge is maintained at a constant level. The coupling constant between the level of hormones and the oscillatory system determines at which number of travelling waves the equilibrium is reached between generation of new oblique lines by branching and their pairwise termination by collision. If this number is low, the pigmented area is small in relation to the total area. The individual oblique lines are the dominating pattern elements. On the other hand, if this number is larger, the pigmented area is also a large proportion of the total so that branchings arise continuously, causing

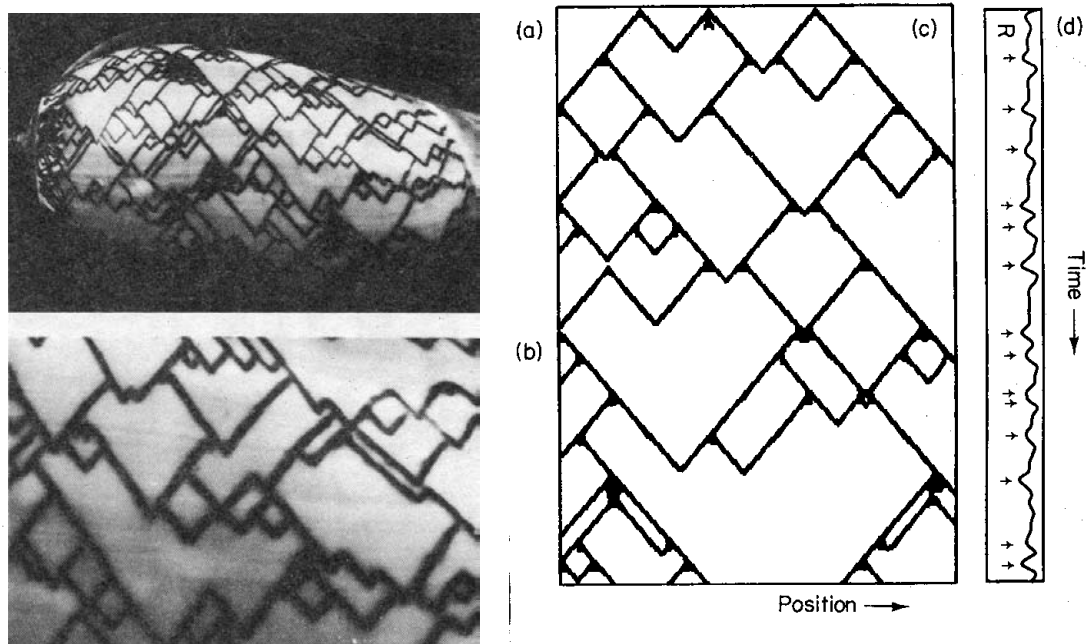


FIG. 8. Formation of branches. (a) and (b) A shell of *Olivia porphyria* L. and details. A branch indicates the sudden formation of a backward wave. (c) and (d) Model: branching occurs whenever the number of travelling waves drops below a certain threshold value. The controlling agent R (d) is a hormone-like substance which is rapidly distributed within the organism and which is produced at a rate proportional to the local activator concentration. R provides thus a measure of how many travelling waves are present. In the simulation shown it is assumed that R inhibits inhibitor decay. Below a certain R concentration (arrows in (d)) the momentarily activated cells switch from the oscillatory mode into a steady state activator production. Groups of cells remain activated longer than the refractory period of their still oscillating neighbouring cells. This initiates backwards waves. Since R is uniformly distributed, branch formation takes place simultaneously on many oblique lines, in agreement with the natural pattern. (Calculated with eqn (2) and $\rho = 0.1$, $\mu = 0.1$, $\kappa = 0.25$, $D_a = 0.015$, $D_h = 0$, $\nu = 0.0014$. Also, it is assumed that $\partial R / \partial t = 0.1 (\sum a/n - R)$, R is uniformly distributed, n : total number of cells; in the simulation shown $n = 260$. In eqn (2), ν is substituted by ν/R and $1/h$ by $1/(0.1 + h)$. A higher ν value would lead to a higher density of lines. In total, 6500 iterations are calculated.

the cells, on average, to remain longer in the steady state mode than in the oscillatory mode.

The overall appearance of the pattern depends also on the ratio between maximum activator production during oscillation and that during steady state activation. If the steady state concentration is low, many cells have to become steadily activated to enable a R -production sufficient to return to the oscillatory mode. This leads to a triangular shaped activation bordered by the original and the branched pigmentation lines. A corresponding simulation based on an activator-substrate model is shown in Fig. 9.

Systems which form branches may also lead to patterns which show regular crossings of pigmentation lines. Since branching occurs simultaneously along the full length of the growing edge due to the overall regulation of the hormone-like substance, and since forward and backward waves have the same inclination with respect to the growing edge, a tendency exists to synchronize the initiations and annihilations of waves. Hence, backward waves are initiated at the same time as

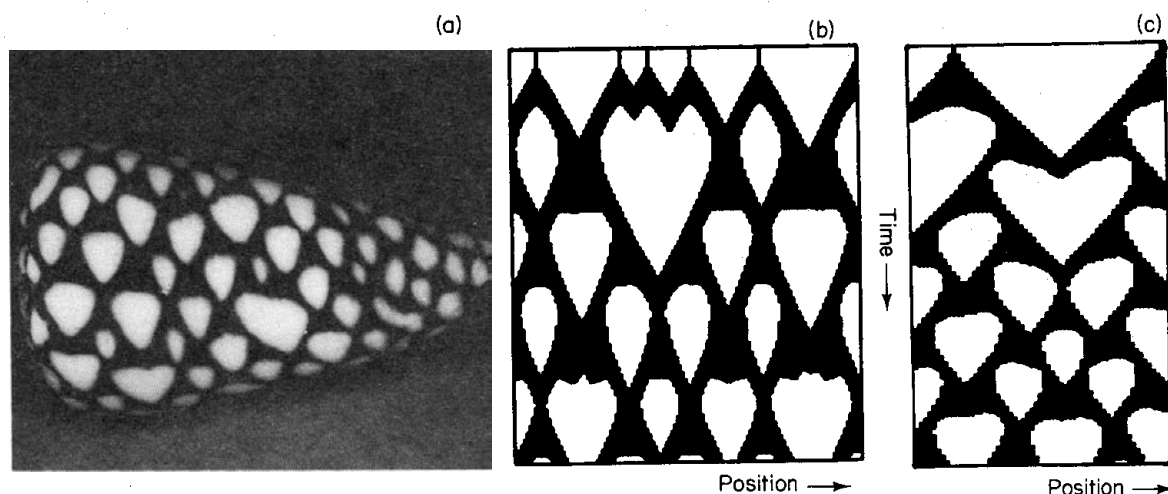


FIG. 9. White triangles on a pigmented background (a) *Conus marmoreus*. (b) Model: assumed is an activator-substrate model (eqn (1)) with the addition that the substrate production is inhibited by a hormone-like substance R . R is produced proportional to the activator concentration. Since R is homogeneously distributed, it is a measure for the average activator concentration. Whenever the number of activated cells drops below a certain threshold, cells are shifted from the oscillatory mode into the steady state mode due to the increased substrate production. In this way branches are initiated. In contrast to the pattern shown in Fig. 8, the region between two newly formed branches becomes pigmented since the steady state activator level is much lower than the peak concentration during oscillation. For this reason, after branch initiation (shift from oscillatory mode to steady state mode) many cells have to enter the steady state activator production in order to shift the system back to the oscillatory mode. Calculated with eqn (1), σ is replaced by σ/R ; $\rho = 0.1 \pm \text{random fluctuation} < 5\%$, $\mu = 0.1$, $\kappa = 3$, $\nu = 0.005$, $\sigma = 0.038$, $D_s = 0$. In addition, $\partial R/\partial t = 0.05 (\sum a/n - R)$; n is the total number of cells (in the simulation shown $n = 69$). Due to the global control via R , the beginning of the white triangles occurs simultaneously. (c) Alternative model: two pattern forming reactions are superimposed (equation not shown). That which causes pigmentation is tuned to produce a steady state activation. A local initiation and the infection leads to a pigmented triangle. Activated cells produce a substrate for a second autocatalytic reaction which switches off the first. After cells have remained for a certain time in the pigment-producing mode, they are forced to switch back. Important is that the switching off reaction spreads out rapidly. This creates the near-simultaneous switching off of many neighbouring cells. Together with the following infection for pigment production from both sides this leads to the unpigmented triangles. This model generates triangles which begin independently and not in synchrony as shown in (b).

many waves disappear following collisions. An indication that crossings are formed by this mechanism would be their regular arrangement and their synchronized appearance. Another mechanism which allows the formation of crossings without global control is discussed in the next section.

Formation of Crossings

Some shell patterns show crossings of pigmentation lines. Such a pattern would arise if, in contrast to the mechanism outlined above, two colliding waves did not extinguish each other. The formation of a crossing can be regarded as the creation of two backwards waves at the moment of collision. As explained already for branch formation, backward waves can arise if groups of cells are shifted from an oscillatory to a steady state activation (pigment production) for a sufficient time such that these cells remain activated until their neighbours have finished the refractory period. This shift has to be induced whenever two waves collide. An example is given in

Fig. 10 where it is assumed that an activator-substrate mechanism is operating with parameters set to enable steady state activation. In addition, it is assumed that the activated cells produce a diffusible inhibitor h (eqns (3a-c)).

$$\frac{\partial a}{\partial t} = \frac{\rho s a^{2*}}{1 + \gamma h} - \mu a + D_a \frac{\partial^2 a}{\partial x^2} \quad (3a)$$

$$\frac{\partial h}{\partial t} = \nu(a - h) + D_h \frac{\partial^2 h}{\partial x^2} \quad (3b)$$

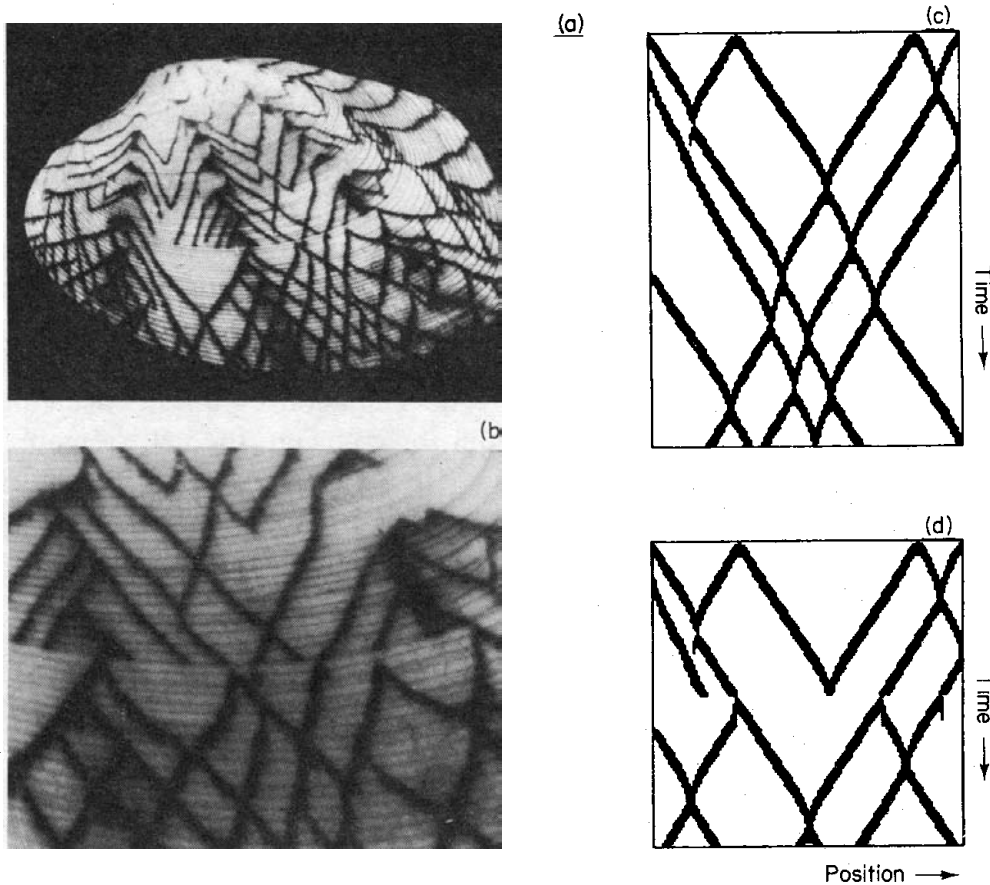


FIG. 10. Crossings of pigmentation lines. (a) and (b) Pattern on *Tapes spec.* and detail. Crossings indicate that two waves do not annihilate each other at a collision but either penetrate each other, or the collision initiates two backwards waves. (c) Model: assumed is a three-component system; an activator-substrate mechanism tuned to produce a steady state activation, plus a diffusible inhibitor (eqn (3)). Travelling waves result from the extinguishing of the steady state activation in each cell by their subsequently triggered neighbouring cells via the diffusible inhibitor. At the point of collision, no new neighbours are available which could provide this inhibition. The cells remain in the steady state until two backwards waves are initiated. (In the simulation, backwards waves are also created after collision with the borders of the field due to the impermeable boundary condition). (d) Pattern regulation: A sudden lowering of the activator concentration to 40% of the actual concentration can lead either to the termination of a line, to branch formation or to the continuation of a line. The same features can be seen in the natural pattern (b). Calculated with eqn (3), $\rho = 0.08 \pm \text{random fluctuations} < 5\%$; $\mu = 0.08$, $D_a = 0.01$, $\kappa = 0.5$, $\gamma = 3$, $\nu = 0.02$, $D_h = 0.4$, $\rho_0 = 0$, $\sigma = 0.1$, $\epsilon = 0.005$, 140 cells, 1800 (c) or 1325 (d) iterations. The random fluctuations allow a different behaviour of the individual waves during the lowering of the activator.

$$\frac{\partial s}{\partial t} = \sigma - \frac{\rho s a^{2*}}{1 + \gamma h} - \epsilon s \quad (3c)$$

where

$$a^{2*} = \frac{a^2 + \rho_0}{1 + \kappa a^2}.$$

This set of equations is, of course, only an example and alternatives are possible. Important is that the autocatalysis is antagonized by two different substances which have different time constants. In addition, one substance must be diffusable, the other not. The formation of crossings would also be possible, for instance, in a system with two inhibitors as long as they fulfill the requirements mentioned above.

The formation of crossings by a system, such as described by eqn (3), should be explained in more detail. Imagine a small activated region: the activation spreads out by a sequence of trigger events very similar to the mechanism described above. The parameters are chosen such that without the influence of the inhibitor the cells would remain in a steady state activation. The resulting pattern would be a growing pigmented triangle. However, due to the diffusible inhibitor, the cells do not remain in the steady state since each subsequently-activated cell extinguishes the activation of the cell which has triggered its activation. The result is travelling waves similar to those discussed above. However, at a point of a collision, the behaviour of the system is different since here there are no neighbours present to extinguish the steady state activation. Thus, at the point of collision, the cells remain activated until the backwards waves are initiated. The newly activated cells extinguish the steady state activation at the point of collision. This sequence of events results in the formation of a cross.

The mechanism of cross-formation as proposed above has some non-trivial regulatory properties that fit well to those observed on shells of *Tapes litteratus* L. On the species shown in Fig. 10, at a particular time many pigment lines become abruptly terminated. However, some lines survive and, frequently, branch immediately after the moment where other lines terminate. Thus, two apparently contradictory processes occur simultaneously: termination of lines and generation of new lines. This behaviour can be explained by the model in a straight-forward manner. We assume that an external event causes a general transient decrease of the activator concentration. This leads to three different patterns: (1) Termination of a line: the activation becomes so low that the chain of trigger events is interrupted. (2) Branch formation: with a somewhat reduced activation, the triggering of neighbouring cells is still possible, but the amount of diffusing inhibitor becomes lower. Cells remain in the steady state long enough to initiate backward waves. The externally reduced activator production mimics the situation which occurs normally during the formation of a crossing. (3) Continuation of a line. This occurs if the activator concentration remains high enough to continue the chain of trigger events, and to extinguish all earlier activated cells. It can be seen in Fig. 10(b) that in some cases incipient branch formation does occur but that the branch becomes rapidly terminated. This detail is also reproduced in the simulation (Fig. 10(d)) and supports our assumption of a diffusible inhibition.

Meshwork-like Patterns

The mechanism outlined above for the generation of crossings is also able to generate other types of patterns which are frequently encountered on shells, for instance meshwork-like or checkerboard-like patterns. These patterns can show transitions into patterns of diagonal lines. Common in these patterns—diagonal lines, meshwork and checkerboards—is that a particular pigmented region is bordered along the space as well as along the time coordinate by non-pigmented regions. The mechanism outlined above for crossings is able to generate these patterns since it is based on an autocatalysis counteracted by *two* inhibitory reactions (which could be realized by a depletion of a substrate, as shown in eqn (3)). One inhibitory substance is highly diffusible and thus responsible essentially for the pattern in space, the other is non-diffusible and responsible essentially for the periodicity of the pattern in time. This is an oversimplification since the actual complexity of the pattern results from the interplay of both inhibitions with the autocatalysis. It is also necessary that both inhibitions have different time constants. Due to the inherent similarities in these patterns minor changes of parameters or even an instability can lead to a transition from one pattern type to another. Such pattern changes are frequently observed on shell patterns of *Bankivia fasciata*. Figure 11 provides some examples together with simulations. The paper of Ermentrout *et al.* (1986) deals more extensively with patterns of this species.

Superposition of Stable and Periodic Patterns

A broad spectrum of patterns on very different species indicates that they are generated by an oscillatory pigment deposition mechanism in which the frequency of the oscillation varies along the growing edge in a systematic manner. This feature is obvious on shells of *Natica enzona* (Fig. 12). Patterns of this type suggest that a spatially stable pattern exists which gives rise to a space-dependent modulation of the oscillation. The outcoming pattern depends on, for instance, whether the spatially stable pattern is periodic or consists of a gradient, or whether the stable pattern only changes the oscillation frequency or subdivides the total field into regions in which oscillatory pigment production, steady state pigment production, or no pigment production at all is possible. Thus, very different patterns can be simulated by using basically the same interaction between the spatially stable pattern and the oscillating system. The spatially stable pattern can be generated by mechanisms such as described by eqns (1) or (2). An example is given in Fig. 3. For the sake of simplicity, in the simulations shown these patterns are not calculated but are numerically introduced. The simulations shown in Figs 12–15 are made with the activator–substrate model (eqn (1)) assuming that the spatially stable pattern influences the substrate production σ . Thus, $\sigma(x)$ is time-independent but depends on the position along the growing edge. In regions in which the substrate production is high, the oscillation frequency is high too. At very high $\sigma(x)$ the cells can enter into a steady state activation. Examples will be given.

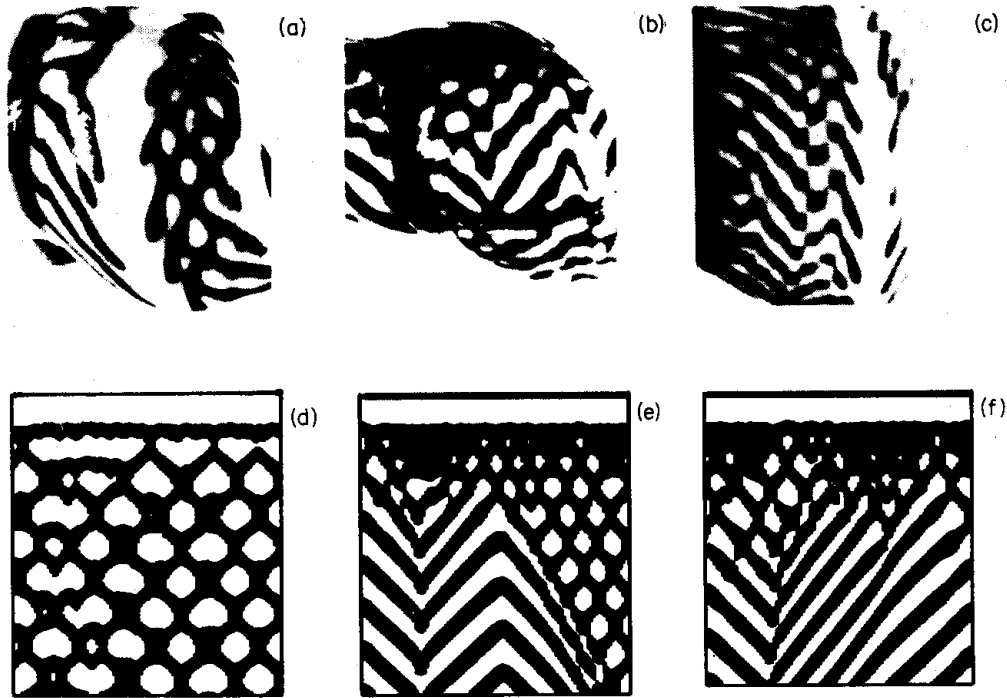


FIG. 11. Meshwork and checkerboard-like pattern. (a)–(c) Patterns on shells of *Bankivia fasciata*. (Photographs kindly supplied by J. Campbell; see Ermentrout *et al.*, 1986.) The patterns can consist of oblique lines of either orientation or in superimposition, forming a meshwork-like pattern. (d)–(f) Model: assumed is one autocatalytic reaction, antagonized by a non-diffusible substrate depleted during autocatalysis plus a diffusible inhibitor (eqn (3)). The first antagonistic reaction causes a periodic pattern in time, the second one a periodic pattern in space. If the time constants of both reactions are different, a tendency to generate meshwork-like patterns exists (d), if they become more similar, the system behaves like a single antagonistic reaction and tends to form travelling waves as discussed above. Intermediate and transient patterns are possible. The simulations reproduce correctly several details of the natural patterns. Travelling waves become retarded shortly before collision (due to the diffusible inhibitor). Somewhat displaced tips of the v-elements results ((b) and (c)). Sharp borders can appear along where pigmented and non-pigmented regions are out of phase ((c) and (f)). Calculated with eqn (3) and $\rho = 0.05 \pm \text{random fluctuation} < 7.5\%$. The random fluctuations are necessary to initiate pattern formation out of homogeneous initial conditions. Further, $\mu = 0.05$, $\rho_0 = 0.005$, $\kappa = 1$, $\gamma = 2$, $S_a = 0.01$, $D_h = 0.4$, $\sigma = 0.03$, $\varepsilon = 0$, $\nu = 0.02$ (a), 0.027 (b), or 0.029 (c).

Formation of Undulating Lines and Partial Synchronization of Cells by Activator Diffusion

Spatial variations in oscillation frequencies can lead to patterns of wavy pigmentation lines. Imagine that initially all cells are in the same phase. This would generate a straight pigment line parallel to the growing edge (see Fig. 5). However, the next pigment production will, due to the effect of the stable pattern, occur in some cells earlier than in others. Thus, the next pigmentation line will have a wavy appearance. With each further oscillation these phase differences will accumulate. After some oscillations, the resulting phase difference between neighbouring cells would be very high. The corresponding patterns would consist of pigmentation lines nearly perpendicular to the growing edge. A natural pattern and a simulation is shown in Fig. 12(a) and (c).

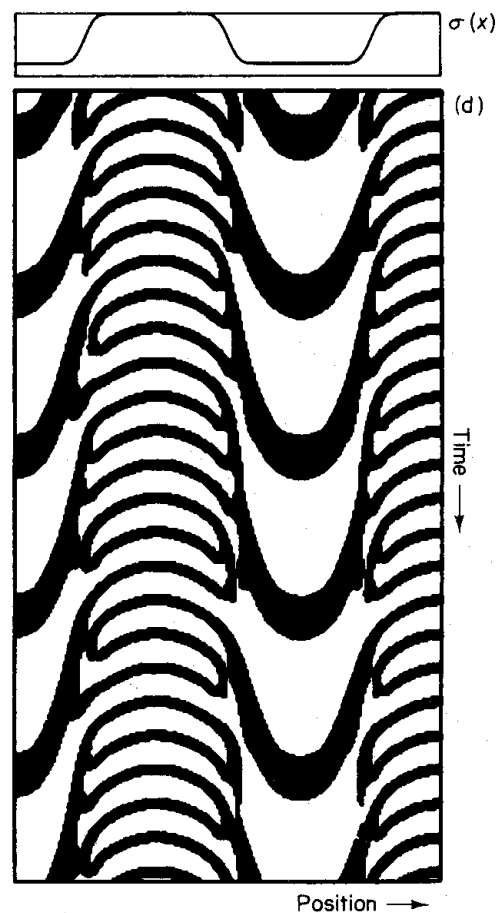
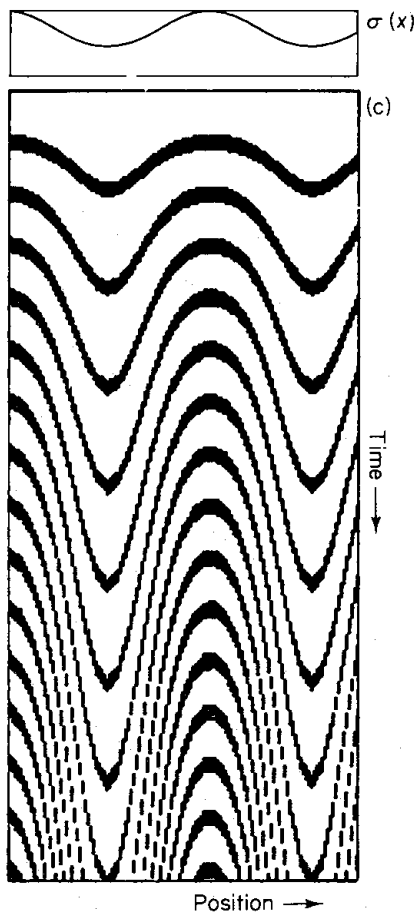
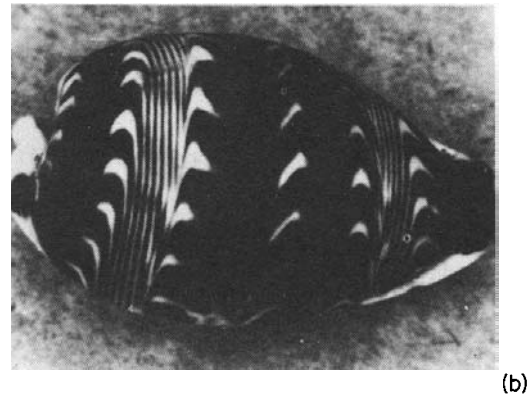


FIG. 12. Superposition of stable and periodic pattern. (a) Shell of *Palamadusta diluculum*. The stripes nearly perpendicular to the growing edge indicate a large phase difference between neighbouring cells. (b) Shell of *Natica enzona*. The oscillation frequency is much higher in some stripes in comparison to the intervenient regions, indicating the existence of a spatially stable pattern which influences the oscillation frequency. (c) and (d) Model: the substrate production (σ in eqn (1)) is assumed to be a function of position ($\sigma(x)$). Regions with higher substrate production oscillate more rapidly. With little or no activator diffusion (c), higher and higher phase differences accumulate between neighbouring cells. The resulting pattern consists of steep thin pigment lines similar to the pattern shown in (b). Calculated with eqn (1) with $\rho = 0.25$, $\kappa = 1$, $\mu = 0.1$, $D_a = 0$, $\rho_0 = 0.004$, $\sigma = \sigma(x)$, as shown, maximum value = 0.031 , $\nu = 0$, $D_s = 0$. A more step-like stable pattern leads to bands with different oscillation frequencies like those shown on shell (a). $\rho_0 = 0.01$, $\kappa = 0.2$, $D_a = 0.015$, $D_s = 0.05$, σ as shown, maximum value = $0.05 \pm$ random fluctuations $< 5\%$. To obtain a correct simulation of the pattern shown in (a), it was necessary to assume that in addition to σ also the other parameters influencing oscillation frequency are under control of the stable pattern, thus μ and ρ have the same spatial pattern as σ , maximum values = 0.1 .

Diffusion of the activator counteracts an increasing accumulation of phase differences between neighbouring cells since a newly activated cell can advance a delayed neighbour by activator exchange. High diffusion of the activator enforces in this way the synchronization of the oscillations, resulting in a pattern which consists of lines more or less parallel to the growing edge (Fig. 5). More interesting patterns result under the influence of a moderate activator diffusion. Travelling waves are periodically initiated in regions of the highest oscillation frequency (high

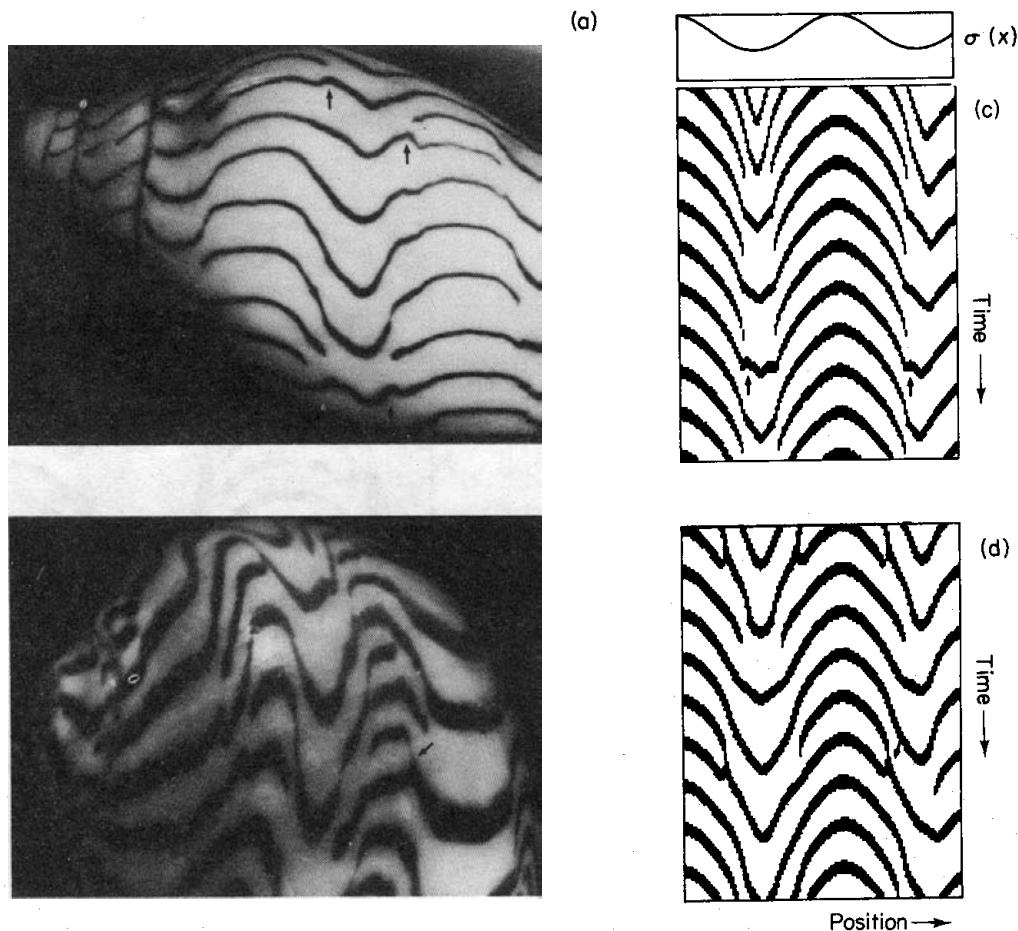


FIG. 13. Wavy lines. (a) Shell of *Amorina undulata*. (b) Shell of *Natica enzona*. (c) and (d) Simulations: Parameters and the assumed stable periodic pattern are the same as in Fig. 12(c), except for the diffusion rates. (c) A moderate activator diffusion ($D_a = 0.015$) enforces a reduction of the phase difference among neighbouring cells. If the phase difference is not too large, a newly activated cell can activate its somewhat delayed neighbours. The steepness of the lines is an indication of the readiness of a cell to become activated. If the phase difference becomes too big, a trigger of the neighbouring cells is not possible; the pigmentation line terminates abruptly. These cells skip one oscillation. Due to the long period without trigger, a spontaneous activation can occur, in agreement with the natural pattern (arrows in (a) and (c)). (d) If, in addition to activator diffusion, some substrate diffusion takes place ($D_s = 0.03$), a connection of a line with the next following line is possible. Due to the substrate supply from the surrounding cells, the activation can be maintained nearly locally. The travelling waves can come to rest without extinction. This "surviving" activation triggers the activation of the surrounding cells as soon as they become susceptible. The resulting pattern consists of a near-perpendicular line which forms a connection with the following pigmentation line. The simulated and the natural pattern agree even in very fine details (arrows in (b) and (d)).

substrate production). They spread into regions of low oscillation frequencies where pairwise annihilation takes place. However, a travelling wave can proceed only if the phase difference between neighbouring cells is not too large. The cell to be triggered must be in the sensitive phase in order that the addition of small amounts of activator releases the autocatalytic burst. For the activator-substrate model, this means that the substrate concentration must have a certain level. Otherwise the chain of trigger events will be interrupted with the consequence that a pigment line becomes terminated. A shell with such a pattern is shown in Fig. 13(a). The model outlined above is able to mimic non-trivial details of this pattern. If a pigment line terminates, the adjacent cells are not activated for a prolonged period. The result is a local gap in the series of pigmentation lines. After a longer time interval without an external trigger, spontaneous activation is possible. This causes a deformation along the first pigmentation line after the gap. Such a wriggle is only expected if a termination of pigment lines has occurred earlier and should be located precisely at the position where the prior line termination took place. Figure 13(a) and (c) shows this pattern on a shell and its reproduction by simulation. This phenomenon has much in common with the pattern regulation shown in Fig. 7(a) and (c).

Interconnections of Wavy Lines

In some species, undulations of pigment lines lead occasionally to connections with a subsequent line. An example is given in Fig. 13(b). As a rule, these connecting lines are steep and very thin. The steepness indicates that the speed of the travelling waves in such regions becomes very slow.

According to the model, interconnections are possible if the antagonistic substance, the substrate or the inhibitor, diffuses at a moderate rate. Given this condition, the chain of trigger events will not necessarily be interrupted if the phase difference between neighbouring cells becomes large. Instead, activation can persist locally since the activation is additionally supported by the influx of substrate from the surrounding cells or by loss of inhibitor into the surrounding cells. During such local persistence of activation, the neighbouring cells advance in their phase until a new chain of trigger events is initiated from these zones of surviving activations. The initiation of new waves of pigmentation by the faint, nearly perpendicular pigmentation lines is clearly visible on the shell shown in Fig. 13(b) and correctly reproduced in the simulation.

Pattern on the Shell of *Nautilus pompilius*

The pattern on the *Nautilus* shell is dominated by the much stronger growth at the one side of the growing edge. This different growth rate generates the spiral-shaped shell. Growth lines on the surface of the shell allow one to determine the position of the growing edge in the course of the animal's individual history (Saunders, 1984). Two such lines are enhanced on the shell shown in Fig. 14(d). Their distance corresponds to a life span of about 2 years. Within this life span eight pigmentation lines have formed on the outer region of the shell while only three have formed on the inner region. This indicates a much higher oscillation frequency at the outer side. The stable pattern which controls oscillation frequency must

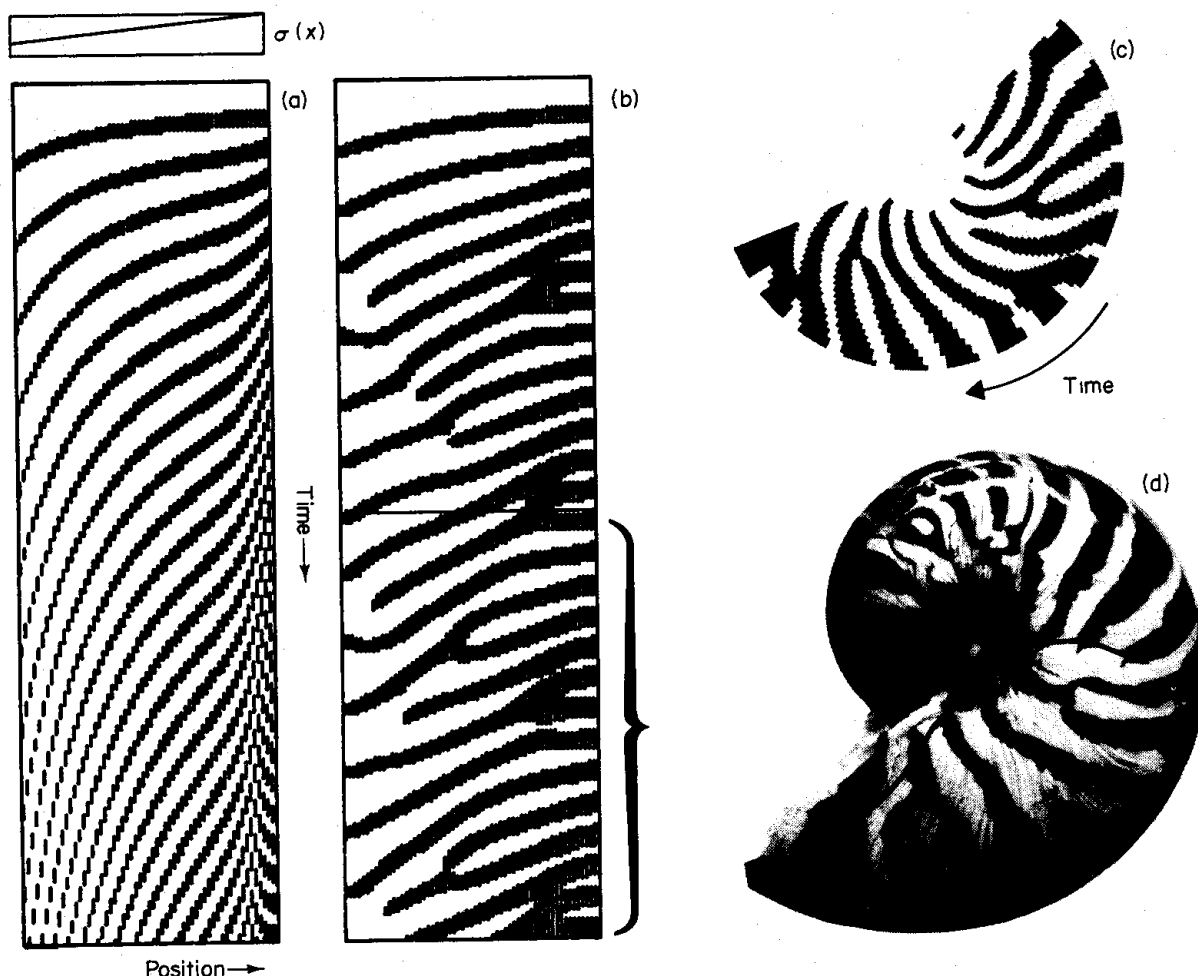


FIG. 14. Pattern on shells of *Nautilus pompilius*. (a)–(c) Model: assumed is an activator–substrate model with a linearly graded substrate production $\sigma(x)$. The oscillation frequency is higher in regions of higher σ . (a) Without diffusion of the activator, this leads to increasing phase differences between neighbouring cells and thus to lines which become steeper and steeper. (b) A moderate activator diffusion leads to a partial synchronization among neighbouring cells. Two pigmentation lines can fuse or pigmentation lines can terminate (see also Fig. 13). Calculated with eqn (1) and $\rho = 0.5$, $\mu = 0.1$, $\rho_0 = 0.004$, $\kappa = 1$, $D_a = 0.1$, $\sigma = 0.012$ – 0.038 , $\nu = 0$, $D_s = 0.1$; 60 cells, 3000 iterations. (c) To show the similarities between the natural pattern and the simulation, the pattern bordered in (b) is drawn as parts of circles. The σ -gradient may also be used to maintain the higher growth rate on one side to achieve the spiral shape of the shell. (d) Shell of *Nautilus pompilius*. The two heavy lines indicate two growth lines at about two years distance.

therefore have a graded distribution. For sake of simplicity, in the simulation (Fig. 14) a linear gradient has been assumed. To obtain the spiral shape of the shell, a similar gradient in the growth rate is required. Both oscillation frequency and growth rate may be under the control of the same gradient.

The pattern on the Nautilus shell shows similar pattern elements as discussed in the previous section: interconnections of successive pigmentation lines and terminating lines which are restricted to the region of high oscillation frequency. It is thus tempting to use a similar mechanism as outlined above. The similarity between the simulated and the natural pattern becomes especially striking if the activator produc-

tion is plotted on parts of concentric circles corresponding to the mode of shell growth.

Superpositions of Oscillating and Non-oscillating Patterns

The patterns obtained have a very different appearance if a stable pattern shifts groups of cells into a permanent steady state. The permanent pigment production of these cells leads to stripes parallel to the direction of growth. The cells in between these stripes are still able to oscillate. Travelling waves are initiated at regular time intervals by the permanently activated cells. The resulting pattern has a fish-bone-like appearance. Between two stripes of permanent pigment production nestled V's are formed. Figure 15 shows a simulation together with a shell of *Palmadusta ziczac* for comparison.

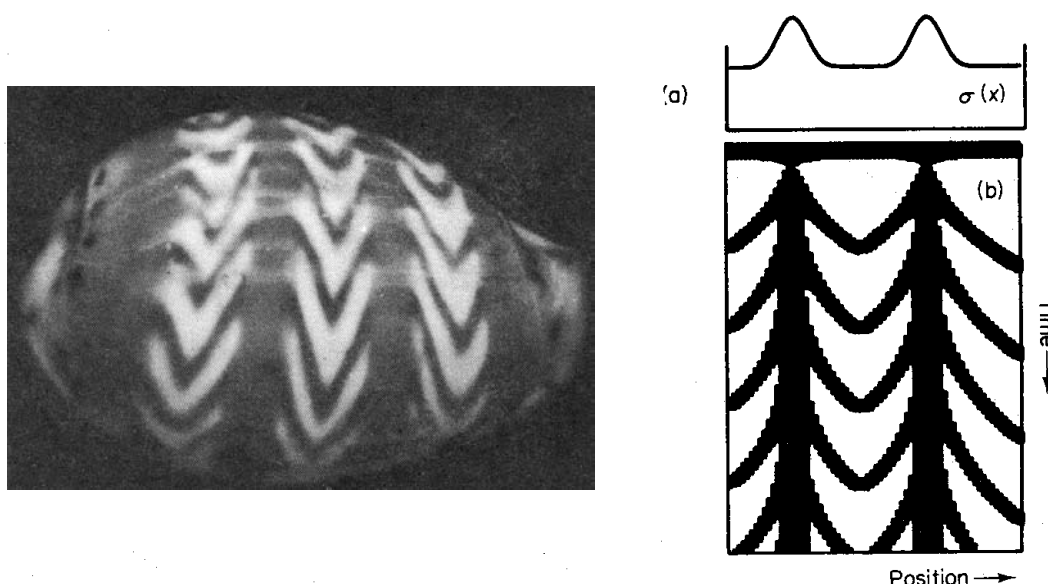


FIG. 15. Fish-bone like pattern resulting from the combination of permanent and oscillatory pigment deposition. (a) Shell of *Palmadusta ziczac*. (b) Model: assumed is an activator-substrate model. In regions where substrate production $\sigma(x)$ is high, cells enter into a steady state activation, causing the pigmented bands parallel to the direction of growth. These permanently activated cells initiate periodically waves travelling into the space between these bands. The wave annihilate each other pairwise at the point of collision (v-elements). Calculated with eqn (1) with $\rho = 0.1$, $\kappa = 0.5$, $\mu = 0.1$, $D_a = 0.01$, $\sigma_{\max} = 0.09$, $D_s = 0.05$, $\nu = 0.002$.

A related pattern is even more frequent: stripes without pigmentation alternate with stripes in which oscillatory pigment deposition takes place (Fig. 16(a) and (b)). In the simulation (Fig. 16(c) and (d)) an activator-inhibitor system is assumed. The spatially stable pattern is assumed to have an additional inhibitory effect on the autocatalysis. This leads to a suppression of oscillation in the high regions of the stable pattern. Depending on the diffusion rates of the involved substances, the patches can have a rounded or crescent-like shape. Both shapes can be found in nature (Fig. 16). The pattern on the shell shown in Fig. 16(a) indicates that the spatially stable pattern is still able to regulate and to adapt to the increasing size

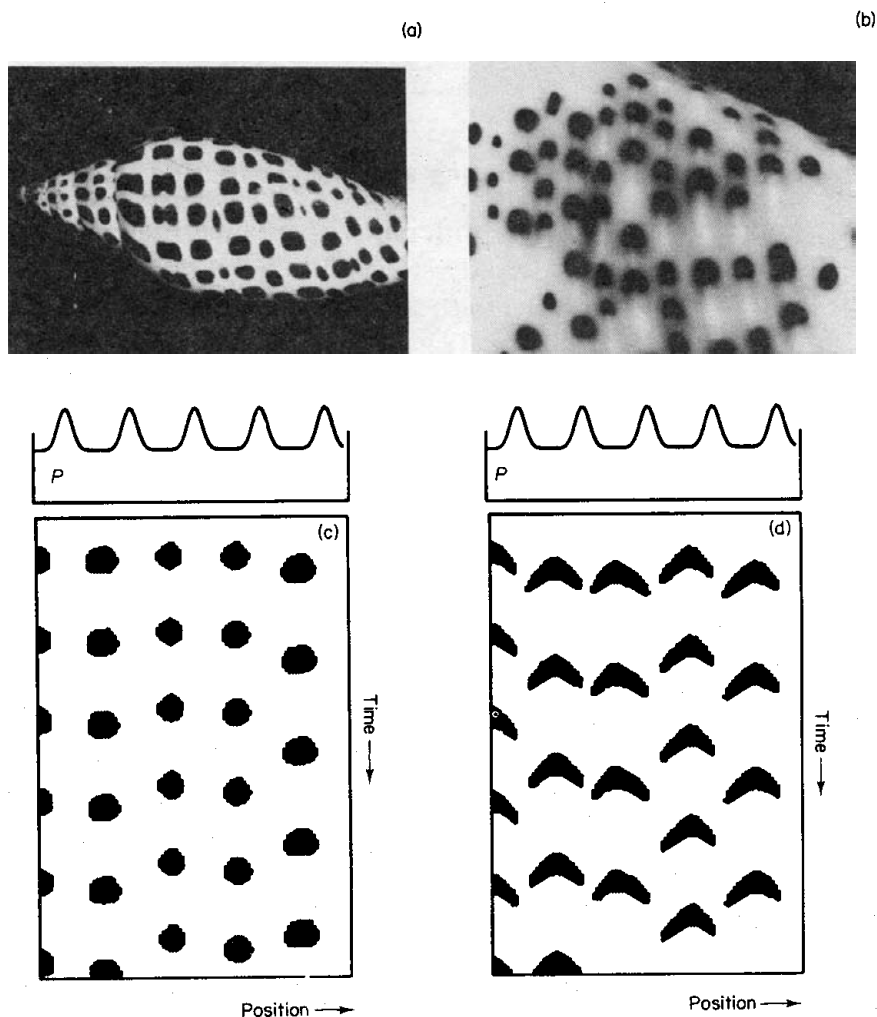


FIG. 16. Rows of patches. (a) *Voluta junonia johnstonae*. (b) Crescent-like patches on *Conus stercus muscarum*. (c) and (d) Model: assumed is an oscillating activator-inhibitor system. The spatial stable system $P(x)$ has an additional inhibitory influence on the autocatalysis ($1/h$ in eqn (2) is replaced by $1/(h + P)$ which suppresses activation in regions of high P). The P -pattern could be generated by a mechanism such as shown in Figs 3 and 4. If the activator and the inhibitor diffuse, rounded patches emerge. (c) If only activator diffuses, the patches obtain a crescent-like shape. Calculated with eqn (2), $\rho = 0.05 \pm \text{random fluctuation} < 5\%$, $\mu = 0.05$, $\rho_0 = 0.02$, $D_a = 0.03$, $\nu = 0.03$, $D_b = 0.1$ (c) and $D_b = 0$ (d); $P_{\max} = 0.41$.

of the cell: a new row of patches is inserted and an existing one splits into two (compare with Fig. 4).

The simulations in Fig. 16 are based on the assumption that the stable pattern has emerged independently from the periodic pattern. An alternative is that the periodic pattern generates its own stable pattern by a positive feedback of the activation on the source density (ρ in eqns (1) and (2)), i.e. on the general ability of a cell to perform the autocatalysis. If in an oscillatory system (as shown for instance in Fig. 5) the antagonistic substance is highly diffusible (lateral inhibition in space), a tendency exists for the lines of activation to disintegrate into individual peaks, but these peaks are not well separated. However, if this sloppy pattern has a long-lasting influence on the source density, the regions of slightly enhanced

activation will obtain a stronger advantage on the next oscillation and so on until a stable periodic pattern in the source distribution is established. It should be mentioned that a very similar feedback of the activator pattern on its source density has to be assumed for the generation of polarity in hydra tissue (Meinhardt & Gierer, 1974).

Shell Patterns Generated by a Two-dimensional Pattern Formation Process

Some mollusc species obtain a completely new pattern during adult life. These patterns are apparently not "space-time plots" but result from a two-dimensional patterning process. Here, the pattern is generated on the surface of the mollusc. The animal engulfs its own shell. The shell obtains a copy of this two-dimensional pattern (a "blueprint"). As a rule, these patterns consist of pigmented patches on a non-pigmented background or vice versa. Figure 17 shows an example in which the juvenile and the adult patterns are visible on the same shell.

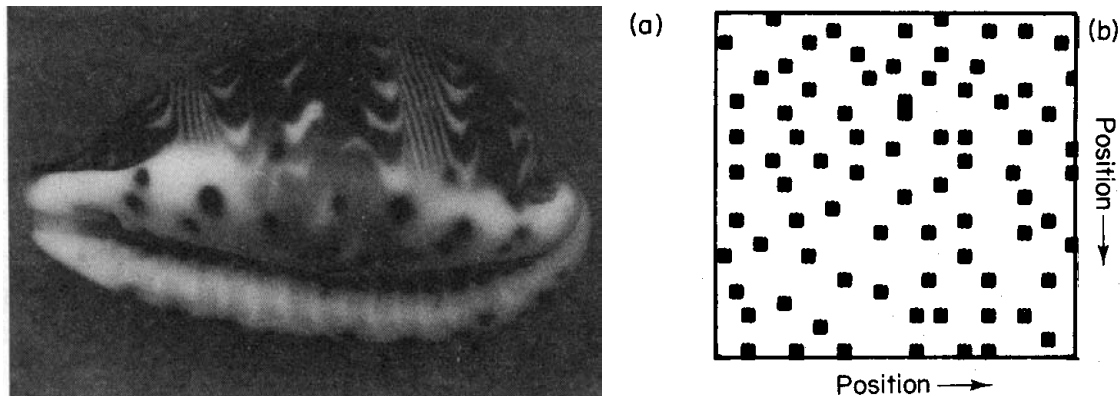


FIG. 17. Two-dimensional pattern formation on shells. Some species obtain, during adult life, a completely different pattern, consisting, as a rule, of spots of pigment or of similarly arranged non-pigmented regions in a pigmented background. These patterns are generated by a two-dimensional pattern formation process and not, as in the normal shells, by a time record of one-dimensional patterning processes. (a) Shell of *Palmdusta diluculum*. The juvenile pattern is still visible and has been discussed already in Fig. 12. The adult pattern consists of somewhat irregularly arranged patches. (b) Model: The same types of interactions (eqns (1) and (2)) used to generate the space-time pattern on normal shells can produce a corresponding pattern of activation in a two-dimensional cell sheet. The distance between the activator maxima is somewhat irregular. Calculated with eqn (2); $\rho = 0.01 \pm$ random fluctuations $< 2.5\%$, $\mu = 0.05$, $D_a = 0.002$, $\nu = 0.07$, $D_h = 0.19$.

Despite the fact that both patterns look so very different they can be explained on the basis of the same interactions. In two dimensions, with appropriate parameters, the mechanism of autocatalysis and lateral inhibition (eqns (1) and (2)) leads to somewhat irregularly spaced activator maxima which correspond well with the irregular arrangement of patches on the shell.

Discussion

The patterns on shells of molluscs show an overwhelming diversity. In an earlier paper (Meinhardt, 1984) it was shown that the basic shell patterns—pigment lines

parallel, perpendicular or oblique to the growing edge—can result if pigment deposition is under the control of an autocatalytic reaction which is antagonized by an inhibitory substance. In the present paper we have shown that more complex patterns can be generated if more than one inhibitory substance is involved or if two patterning processes are superimposed and interfere with each other. The patterns generated by the model agree well with the natural patterns and even fine details are correctly reproduced. In addition to the pattern itself, the model also accounts for pattern regulation such as observed on some specimens after presumed external perturbations. In this way, the model is superior to any cell automata model which would require a different set of rules for pattern formation and regulation. It should be emphasized that the correct description of the details and regulatory processes does not result from special adaptations of the model but follows from the general mode of pattern formation in a straightforward way (see, for instance, Fig. 7 and 10). Minor changes of parameters can lead to very different patterns, providing a rationale for the diversity of patterns in closely related species or even on different specimens of the same species.

The model proposed is based on interactions developed for the description of patterning processes during development of higher organisms (Gierer & Meinhardt, 1972; Meinhardt, 1982), for instance, for the generation of positional information. The fact that the same interactions also can account for shell patterning indicates that the shell patterning process is a special case of a general pattern formation process.

Although the model describes very different patterns with a high degree of accuracy, we have been unable so far to provide a computer simulation for some important classes of patterns. For instance, on some species, instead of oblique lines the shell patterns consist of a sequence of triangles. (The paper by Lindsay (1982) is devoted to this problem). A close inspection of the pigment lines of Fig. 1(e) shows this feature at a minute scale. Triangles originate if, by infection, more and more cells switch from the oscillating into the steady state mode but switch back to the oscillating mode just at once. Triangle formation is very reminiscent of the initial steps in branch formation (see Figs 8 and 9) except that ultimately only the original travelling wave survives.

Another pattern not yet simulated is that of *Conus textile* (Fig. 1(g)). It consists of nested U-patterns with U's of very different sizes. The rounded shape of the U's indicates increasing speeds of the travelling waves. In principle, the model can account for this speeding up due to the increasing susceptibility of the cells with increasing time after the last activation (the bending of the lines in Fig. 7 has this origin). The problems in the attempt to simulate the *Conus*-pattern result from the different sizes of the U's, indicating that this speeding up can take place at very different time intervals after the last activation. An alternative reason for the U shapes could be a mutual attraction of two approaching travelling waves. This, however, is in conflict with the separation of two waves after branch formation. Nevertheless, there are also similarities of these two patterns with those simulated, what suggests that these patterns do not represent a completely different class of pattern but require some yet unknown modifications.

Very little is known about the biological basis of shell patterning. In principle, the interactions in the model proposed are compatible with other than biochemical realizations, including lateral inhibition on a neuronal basis such as proposed by Ermentrout *et al* (1986). In this case the model would only describe the logic behind the process. Nevertheless, it seems more likely to us that a process is involved which depends on a limited amount of substances which mutually regulate their production rate and which become distributed in the organism either by diffusion or convection. We hope that this modelling provides a better understanding of the molecular basis of shell patterning.

We thank Prof. A. Seilacher and Dr A. Roll for mollusc species, J. Campbell and G. Oster for the communication of their results prior to publication and B. Nagorcka for a critical reading of the manuscript.

REFERENCES

- ERMENTROUT, B., CAMPBELL, J. & OSTER, G. (1986). *Veliger* **28**, 369.
GERISCH, G. (1968). *Curr. Top. Dev. Biol.* **3**, 157.
GIERER, A. & MEINHARDT, H. (1972). *Kybernetik* **12**, 30.
LINDSAY, D. T. (1982). *Differentiation* **2**, 32.
MEINHARDT, H. (1982). *Models of biological pattern formation*. London: Academic Press.
MEINHARDT, H. (1984). *J. Embryol. exp. Morph.* **83**, Supplement 289.
MEINHARDT, H. & GIERER, A. (1974). *J. Cell Sci.* **15**, 321.
MEINHARDT, H. & KLINGLER, M. (1987). *Lecture notes in Biomathematics* (in press).
SEILACHER, A. (1972). *Lethaia* **5**, 325.
SEILACHER, A. (1973). *Sys. Zoo.* **22**, 451.
SAUNDERS, W. B. (1984). *Science* **224**, 990.
WADDINGTON, C. H. & COWE, J. (1969). *J. theor. Biol.* **25**, 219.